BMC Medicine

RESEARCH

Open Access

Estimation of physiological aging based on routine clinical biomarkers: a prospective cohort study in elderly Chinese and the UK Biobank

Ziwei Zhu[1,2], Jingjing Lyu[1,2], Xingjie Hao[1,2], Huan Guo[1,3], Xiaomin Zhang[1,3], Meian He[1,3], Xiang Cheng[4], Shanshan Cheng[1,2*] and Chaolong Wang[1,2*]

Abstract

Background Chronological age (CA) does not reflect individual variation in the aging process. However, existing biological age predictors are mostly based on European populations and overlook the widespread nonlinear effects of clinical biomarkers.

Methods Using data from the prospective Dongfeng-Tongji (DFTJ) cohort of elderly Chinese, we propose a physiological aging index (PAI) based on 36 routine clinical biomarkers to measure aging progress. We first determined the optimal level of each biomarker by restricted cubic spline Cox models. For biomarkers with a U-shaped relationship with mortality, we derived new variables to model their distinct effects below and above the optimal levels. We defined PAI as a weighted sum of variables predictive of mortality selected by a LASSO Cox model. To measure aging acceleration, we defined ΔPAI as the residual of PAI after regressing on CA. We evaluated the predictive value of ΔPAI on cardiovascular diseases (CVD) in the DFTJ cohort, as well as nine major chronic diseases in the UK Biobank (UKB).

Results In the DFTJ training set (n = 12,769, median follow-up: 10.38 years), we identified 25 biomarkers with significant nonlinear associations with mortality, of which 11 showed insignificant linear associations. By incorporating nonlinear effects, we selected CA and 17 clinical biomarkers to calculate PAI. In the DFTJ testing set (n = 15,904, 5.87 years), PAI predict mortality with a concordance index (C-index) of 0.816 (95% confidence interval, [0.796, 0.837]), better than CA (C-index = 0.771 [0.755, 0.788]) and PhenoAge (0.799 [0.784, 0.814]). ΔPAI was predictive of incident CVD and its subtypes, independent of traditional risk factors. In the external validation set of UKB (n = 296,931, 12.80 years), PAI achieved a C-index of 0.749 (0.746, 0.752) to predict mortality, remaining better than CA (0.706 [0.702, 0.709]) and PhenoAge (0.743 [0.739, 0.746]). In both DFTJ and UKB, PAI calibrated better than PhenoAge when comparing the predicted and observed survival probabilities. Furthermore, ΔPAI outperformed any single biomarker to predict incident risks of eight age-related chronic diseases.

Conclusions Our results highlight the potential of PAI and ΔPAI as integrative biomarkers to evaluate aging acceleration and facilitate the development of targeted intervention strategies for healthy aging.

*Correspondence:
Shanshan Cheng
sscheng@hust.edu.cn
Chaolong Wang
chaolong@hust.edu.cn
Full list of author information is available at the end of the article

Keywords Biological age, Clinical biomarker, Mortality, Nonlinear association, Aging

Background

Population aging has imposed a heavy health burden, as well as potential economic and societal costs, with substantial increase occurring in developing countries [1]. It has been known that for individuals of the same chronological age (CA), those with obesity, long-term nicotine exposure, or lower socioeconomic status are more likely to experience adverse health outcomes and increased mortality risk [2]. Thus, it is important to measure one's biological age (BA) to identify individuals with accelerated aging and to develop precision prevention and intervention strategies for major chronic diseases in an aging population.

To date, researchers have developed a variety of predictors of BA using biomarkers such as telomere length, DNA methylation [3–6], gene expression [7, 8], metabolites [9], or clinical biomarkers [5, 10, 11]. While BA indices based on genomic data, such as DNA methylation, are accurate in predicting CA [6, 12], clinical biomarkers are generally more affordable, interpretable, and modifiable. Putin et al. have developed a deep neural network model to predict CA based on electronic medical records, covering 46 routine clinical biomarkers [11]. The Klemera and Doubal's method (KDM) [13], which assigns weights to biomarkers based on their associations with CA, has been widely used to estimate BA, including the BioAge derived from the NHANES III data [14]. In addition, Chen et al. have proposed KDM-BA based on 12,377 individuals from the China Kadoorie Biobank (CKB) and validated its association with all-cause mortality [15]. However, these predictors were primarily based on supervised models with CA as the training label and thus may have limited value to predict disease risks independent of CA [16–18].

To address the limitation, some studies proposed predictors of mortality risk, assuming that the survival time reflects one's BA [17, 18]. For example, GrimAge [3], PhenoAge [4], and DOSI [10] were trained to predict mortality risk based on DNA methylation or clinical biomarkers. These models, however, were mostly based on European populations and linear assumptions. Given the population heterogeneity in genetic and environmental factors, aging patterns in Europeans might be distinct from those in East Asians [19]. Moreover, existing models have overlooked the widely reported U-shaped relationships between clinical biomarkers and mortality [20–22].

In this study, we propose a physiological aging index (PAI) based on 36 clinical biomarkers from the Dongfeng-Tongji (DFTJ) cohort of elderly Chinese [23] (Fig. 1). PAI aims to measure an individual's BA based on routine clinical biomarkers in the blood. We use restricted cubic spline (RCS) Cox models to capture potential U-shaped relationships between clinical biomarkers and mortality, and determine the optimal value of each biomarker for subsequent piece-wise linear transformation. We define PAI as a linear combination of CA and the transformed biomarkers, as well as ΔPAI as the residual of PAI after regressing on CA. Thus, ΔPAI measures physiological aging acceleration independent of CA. We evaluate the predictive value of PAI and ΔPAI on mortality and incident cardiovascular diseases (CVD) in the DFTJ cohort, as well as on mortality and nine chronic diseases in the UK Biobank (UKB). With PAI and ΔPAI, we might identify individuals at high risk of accelerated aging and provide targeted interventions to improve their health outcomes.

Methods

Study population

This study was based on the DFTJ cohort of retired employees from the Dongfeng Motor Company in Shiyan, Hubei, China [23]. DFTJ cohort recruited 27,009 participants in 2008 and have completed two follow-up visits in 2013 and 2018. In 2013, 24,175 participants were followed up and 14,120 participants were newly enrolled (Additional file 1: Fig. S1) [4, 24–30]. All participants completed both face-to-face questionnaires and physical examinations in eight hospitals after an over-night fasting. We used samples recruited in 2008 from the Zhongxin hospital ($n=13,555$) as the training set, and samples newly recruited or followed up in 2013 from Zhongxin ($n=15,956$), Tianai ($n=1971$), Huaguo ($n=4585$), and Maojian ($n=4478$) hospitals as the testing set. We excluded participants from hospitals with high missing data rates (>50%) in at least 5 variables among the 36 clinical biomarkers included in this study (Additional file 1: Table S1). The cohort entry date is defined as the date of blood collection for each participant.

All participants provided written informed consent. The study protocol was approved by the Medical Ethics Committee of Tongji Medical College, Huazhong University of Science and Technology.

Clinical data

Lifestyles, health and medication history, and family history were assessed using structured questionnaires. Anthropometric measures and blood tests included biomarkers related to cardiometabolic, hematological, hepatic, and

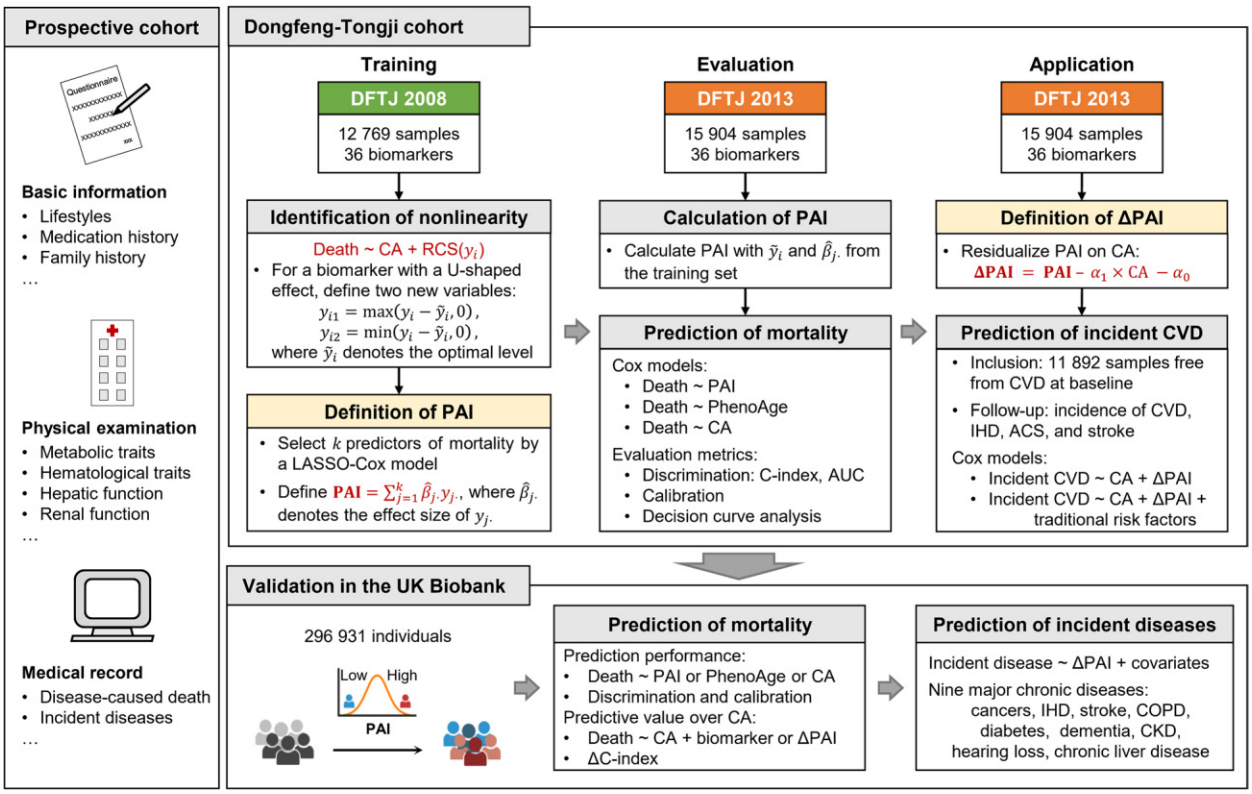

Fig. 1 Overall study design

renal function (Additional file 1: Table S1). Lifestyle factors such as smoking and drinking status, diet, sleep duration, and exercise frequency were defined according to previous studies [25, 27]. Prevalent diseases, including cancers, hypertension, dyslipidemia, diabetes, and cardiovascular diseases, were identified through a combination of self-reported medical history and blood tests. A detailed description of this clinical information is provided in Additional file 1: Supplementary methods.

Outcome definition

The primary outcome was death events until May 20, 2019. Causes of death were defined based on the International Classification of Diseases Tenth Revision (ICD-10) [31]. For survival analyses, we excluded accidental deaths (ICD-10 codes: V01-Y98). All participants were regularly followed up from enrollment by trained staff blind to sample characteristics through electronic medical records from the health insurance network of Dongfeng Motor Company [32].

The secondary outcomes were incident CVD events until December 31, 2018, among 31,751 participants, after excluding those with prevalent ischemic heart disease (IHD, $n=5468$), stroke ($n=1972$), cancer ($n=2182$), or severely abnormal electrocardiogram ($n=674$, including atrial fibrillation, atrial flutter, pre-excitation syndrome, pacemaker rhythm, and frequent premature ventricular contractions) at baseline, and those lost to follow-up ($n=709$) [33]. CVD diagnosis was done by physicians following the standard of the American Heart Association[34]. CVD included IHD (ICD-10: I20–I25) and stroke (I60, I61, I63, I64, I69.0, I69.1, I69.3, and I69.4). Acute coronary syndrome (ACS), the most severe subtype of IHD, was defined by ICD-10 I20.0 and I21 (Additional file 1: Table S2).

Quality controls

In the training set, we started with 13,555 samples and 36 clinical biomarkers collected in 2008 (Additional file 1: Fig. S2). First, we removed 727 samples with prevalent cancer and 35 samples with > 5 missing biomarkers. Next, we performed log-transformation of right-skewed variables with skewness > 1.5 and further removed 24 samples with outlier measurements defined as > 8 interquartile range (IQR) from median (Additional file 1: Fig. S3A). We used the predictive mean matching method to impute missing values (Additional file 1: Fig. S3B) based on clinical biomarkers and age[35]. We performed multiple imputation for 5 times, each with 10 iterations, and took the mean of the imputed values. The final training set included 12,769

samples, of whom 1763 died during a median follow-up of 10.38 years.

Similar quality controls were applied on the testing set. The testing set initially included 26,990 samples and 36 biomarkers collected in 2013 (Additional file 1: Fig. S4). We first removed samples with prevalent cancer ($n=1044$), >5 missing variables ($n=153$), or no survival information ($n=10$). After log-transformation of right-skewed variables, we removed 21 samples with extreme outlier measurements (Additional file 1: Fig. S5A) and imputed missing data by multiple imputation (Additional file 1: Fig. S5B). Finally, we excluded 9858 samples that overlapped with the training set and retained 15,904 samples in the testing set, of whom 769 died during a median follow-up of 5.87 years.

Associations of clinical biomarkers and mortality

In the training set, we analyzed both linear and nonlinear associations between 36 biomarkers and mortality. Linear associations were assessed using Cox proportional hazard models, where each model included CA and a clinical biomarker as predictors. Linearity was inspected by applying the Wald test on the regression coefficient. Nonlinear associations were examined using Cox models with cubic splines [36]. We used the *rcs* function from the R package *rms*, setting three knots for each biomarker at the 10th, 50th, and 90th percentiles and adjusting CA as a covariate. Nonlinearity was tested by variance analysis using the *anova* function in R. Associations with $P<0.0014$ (0.05/36) were considered significant.

Model construction

For biomarkers identified to have U-shaped relationships with mortality, we first identified their optimal levels based on the lowest mortality risk on their RCS curves, denoted as $\widetilde{y}_i$ for biomarker i. We then modeled the effects below and above $\widetilde{y}_i$ separately by replacing y_i with two variables y_{i1} and y_{i2}, which were defined as.

$$y_{i1} = \max\left(y_i - \widetilde{y}_i, 0\right),$$

$$y_{i2} = \min\left(y_i - \widetilde{y}_i, 0\right).$$

We kept the original y_i for biomarkers with no U-shaped relationship. Next, we incorporated these variables and CA into a LASSO Cox model to predict mortality. We tuned the hyperparameter λ by fivefold cross-validation with 20 repeats using the *cv.glmnet* function in the R package *glmnet* [37]. We chose the largest λ value for which the partial likelihood deviance was within one standard error of the minimum observed. For the integrity of a biomarker, we kept both y_{i1} and y_{i2} as predictors even when only one was selected by LASSO.

We defined PAI as a linear combination of all selected predictors, weighted by their regression coefficients in the Cox model described above. Following the concept of established aging clocks [4], we further defined ΔPAI as the residual of PAI after regressing on CA. By design, ΔPAI measures accelerated aging deviated from the expected aging trajectory. ΔPAI was normalized to unit variance.

Model evaluation

Based on the DFTJ testing set, we compared the performance of PAI, PhenoAge [4], and CA to predict mortality risk based on Cox models with no covariates. When calculating PhenoAge (Additional file 1: Table S3), we ignored albumin and C-reactive protein because these two biomarkers were not measured in the DFTJ cohort. We evaluated each model by discrimination (Harrell's concordance index [C-index], receiver operator characteristic [ROC] curve) [38, 39], calibration (calibration slope and intercept) [40], and clinical utility (decision curve analysis) [41, 42]. We calculated the time-dependent area under the ROC curve (AUC) for 1-, 3-, and 6-year intervals using R package *timeROC*, of which 95% CIs were computed by 1000 bootstrap repetitions. Calibration slope and intercept were computed by comparing the observed and predicted 6-year survival probabilities. We divided the testing set equally into 10 groups based on the predicted survival probabilities and derived the observed survival probability in each group using the Kaplan–Meier estimator via the *groupkm* function from the R package *rms*. We applied Cox models with ΔPAI and/or ΔPhenoAge as predictors of mortality, all adjusting for CA as a linear covariate, to estimate the mortality risk associated with accelerated aging. The effect size was quantified as HR per standard deviation (SD) increase in ΔPAI or ΔPhenoAge. Given the heterogeneity between hospitals (Additional file 1: Fig. S6, Table S4), we also conducted sensitivity analyses by incorporating hospital as a random effect in the Cox models, using the R package *coxme*.

We evaluated the predictive value of a single biomarker on mortality using fractional polynomials to incorporate nonlinear effects [43]. Prediction of mortality was based on Cox models with CA and fractional polynomial terms of a single biomarker, as implemented by the *mfp* function from the R package *mfp*. We set the degree of freedom (df) to 4 and fractional polynomial selection level (alpha) to 0.01 in the *mfp* function. We computed Harrell's C-index and 6-year interval AUC for each model and compared to the reference model with CA as the only predictor. The increases in C-index (ΔC) than the

reference model were assessed by *Z*-score tests and one-sided *P* values using the R package *compareC* [44]. Statistical significance was defined as $P < 0.0028$ (0.05/18) to account for multiple tests of 17 biomarkers (included in PAI) and ΔPAI.

Prediction of incident CVD in the DFTJ cohort

We evaluated the performance of ΔPAI to predict incident risks of CVD, IHD, ACS, and stroke in the DFTJ testing set. After excluding 4012 samples with prevalent IHD, stroke, cancers, or severely abnormal electrocardiogram at baseline, and those lost follow-ups, we included 11,892 samples for subsequent analyses. We computed the HR per SD increase in ΔPAI using a mixed-effect Cox model with hospital as a random effect. We also stratified samples by quartiles of ΔPAI and computed the HR of each quartile by mixed-effect Cox models, treating the lowest quartile as the reference and the hospital as a random effect. Two sets of models were tested, one including CA as a covariate (base model) while the other set additionally adjusting for sex, hypertension, hyperlipidemia, diabetes, obesity, smoking, drinking, diet, sleep duration, exercise frequency, and family history of the disease of interest (full model). Definitions of these covariates were provided in Additional file 1: Supplementary methods. In models of ACS, we adjusted for the family history of IHD due to a lack of information specifically on ACS. We considered $P < 0.05$ as statistically significant in this analysis.

External validation in the UK Biobank

UKB recruited about 0.5 million participants (aged 37 to 73 years) between 2006 and 2010 from 22 assessment centers in England, Scotland, and Wales, where they completed physical assessments, questionnaires, and blood collection[45]. The summary information of UKB can be accessed through the showcase website (Showcase Homepage). We validated the performance of PAI to predict mortality risk using individual data from UKB (Fig. 1). We defined the outcome as death excluding accidental death (ICD-10 codes: V01-Y98). The cohort entry date was set as the date of blood collection (Field 3166). Participants were followed up until December 31, 2021, death, or deregistration, whichever came first.

Starting with 502,401 samples and 19 clinical biomarkers for PAI and PhenoAge calculation (Additional file 1: Table S1), we performed similar quality controls as the DFTJ cohort. We removed 1298 samples lost to follow-up, 5334 samples failed in blood sample collection in the assessment center, and one sample missing registered death date. Then, we removed 48,117 samples with self-reported (Field ID: 20,001) or medical recorded (Field ID: 41,270, ICD-10 C00-C97) cancers before the cohort entry date. Next, we kept 298,284 samples with no missing clinical biomarkers (Additional file 1: Fig. S7A). After log-transformation on right-skewed variables (Additional file 1: Table S1), we removed 1353 samples with extreme outlier measurements (>8 IQR from median, Additional file 1: Fig. S7B). We calculated PAI and ΔPAI for the remaining 296,931 individuals, among whom 19,684 deaths occurred during a median follow-up of 12.80 years. ΔPAI was normalized to unit variance.

We computed PAI for UKB participants using the model derived from the DFTJ training set. Next, we compared the performance of PAI, PhenoAge, and CA in mortality risk prediction based on Cox models with no other covariate. We calculated time-dependent AUCs for 1-, 3-, 6-, and 12-year intervals and calibration of 12-year intervals. Finally, we evaluated the improvement in mortality risk prediction over CA introduced by ΔPAI and each of the 17 biomarkers following the procedures described in the Model evaluation section.

Prediction of major chronic diseases in the UK Biobank

We assessed the predictive value of ΔPAI on major chronic diseases in the UKB. We selected nine age-related chronic diseases among the top causes of disability-adjusted life-year (DALY) for individuals aged over 55 globally [30], including all cancers, ischemic heart disease (IHD), stroke, chronic obstructive pulmonary disease (COPD), diabetes, Alzheimer's diseases and other dementias, chronic kidney disease (CKD), age-related and other hearing loss, and cirrhosis and other chronic liver diseases. Detailed selection procedures of these diseases are provided in Additional file 1. We tracked disease status until December 31, 2021, using hospital inpatient data from UKB (Field ID: 41,270) [46]. We excluded prevalent cases at baseline using hospital inpatient data and self-reports (Field ID: 20,002, Additional file 1: Table S5). We estimated HR per SD increase in ΔPAI for each disease using Cox models, adjusting for CA, sex, smoking, drinking, obesity, and the Townsend index (TS index). We considered $P < 0.006$ (0.05/9) as statistically significant.

We also compared ΔPAI, ΔPhenoAge, and 17 biomarkers on the incident risk prediction of each disease. We computed the improvement in C-index (ΔC) after adding each of these variables as linear terms to a reference Cox model including CA, sex, smoking, drinking, obesity status, and the TS index as covariates. The significance of ΔC was evaluated using R package *compareC* and we considered $P < 0.0026$ (0.05/19) statistically significant.

Results

Basic characteristics of the study population

The training set included 12,769 individuals (52.1% females), with a mean age of 64.1 (SD = 7.88) years.

Table 1 Basic characteristics of the DFTJ cohort

Variable [a]	Training set			Testing set		
	Survival	Death	*P* [b]	Survival	Death	*P* [b]
	n **= 11,006**	***n*** **= 1763**		***n*** **= 15,135**	***n*** **= 769**	
Sex, female (%)	6067 (55.1)	587 (33.3)	**< 0.001**	8885 (58.7)	250 (32.5)	**< 0.001**
Age, years	63.1 (7.51)	70.0 (7.52)	**< 0.001**	62.2 (8.20)	71.3 (8.41)	**< 0.001**
BMI, kg/m^2	24.5 (3.29)	24.4 (3.61)	0.295	24.1 (3.25)	23.9 (3.68)	0.174
Smoking status, *n* (%)			**< 0.001**			**< 0.001**
Current	1902 (17.3)	939 (53.3)		2505 (16.6)	211 (27.4)	
Former	1232 (11.2)	473 (26.8)		1558 (10.3)	145 (18.9)	
Never	7872 (71.5)	351 (19.9)		11,072 (73.2)	413 (53.7)	
Drinking status, *n* (%)			**< 0.001**			**< 0.001**
Current	2270 (20.6)	1166 (66.1)		3823 (25.3)	179 (23.3)	
Former	608 (5.52)	426 (24.2)		758 (5.01)	79 (10.3)	
Never	8128 (73.9)	171 (9.70)		10,554 (69.7)	511 (66.4)	
Diagnosis, *n* (%)		1174 (66.6)				
Hypertension	5474 (49.7)	902 (51.2)	**< 0.001**	9179 (60.6)	603 (78.4)	**< 0.001**
Hyperlipidemia	4963 (45.1)	558 (31.7)	**< 0.001**	6586 (43.5)	386 (50.2)	**< 0.001**
Diabetes	2048 (18.6)	454 (25.8)	**< 0.001**	2792 (18.4)	273 (35.5)	**< 0.001**
IHD	1596 (14.5)	165 (9.36)	**< 0.001**	2152 (14.2)	222 (28.9)	**< 0.001**
Stroke	390 (3.54)	587 (33.3)	**< 0.001**	659 (4.35)	128 (16.6)	**< 0.001**

[a] Data are presented as mean (SD) for continuous variables and number (percentage) for categorical variables

[b] *P* for values between death events and survivals are derived from Student's *t* test for continuous variables, and chi-square test for the categorical variables

Participants who died during the follow-up were older, more likely to be current smokers or drinkers, and more likely to have metabolic diseases and CVD at the baseline ($P < 0.001$, Table 1). Among 15,904 individuals in the testing set, 57.4% were females with a mean age of 62.7 (8.45) years. Like the training set, participants who died were older, more likely to be current smokers, and patients with metabolic diseases or CVD ($P < 0.001$, Table 1).

Associations between clinical biomarkers and mortality

In the training set, we observed 17 and 25 biomarkers to have linear and nonlinear associations with mortality, respectively, including 14 overlapping biomarkers ($P < 0.0014$, Table 2 and Additional file 1: Fig. S8). Remarkably, we identified 11 biomarkers with strong U-shaped relationships but no significant linear associations with mortality (Fig. 2). In contrast, only three biomarkers, namely red cell volume distribution width (RDW), diastolic blood pressure (SBP), and pressure pulse (PP), showed significant linear but insignificant nonlinear associations with mortality (Additional file 1: Fig. S8).

Prediction of mortality risk in the DFTJ cohort

By applying a LASSO Cox model, we selected CA and 17 biomarkers predictive of mortality, including two biomarkers with linear associations (RDW and SBP) and 15 with U-shaped associations (Additional file 1: Fig. S9). After replacing each nonlinear biomarker with two variables, a total of 33 variables were included in the calculation of PAI, of which weights were estimated by fitting a multivariable Cox model to predict mortality using the training set (Additional file 1: Table S6). PAI was highly correlated with CA in both the training (Pearson's $r = 0.848$) and testing ($r = 0.867$, Fig. 3) sets. By regressing on CA, ΔPAI has a mean of 0 and a SD of 0.60 in the testing set.

In the testing set, PAI consistently outperformed PhenoAge and CA to predict mortality (Table 3). In terms of discrimination, PAI had a C-index of 0.816 (95% CI: 0.802, 0.831), higher than those of 0.799 (0.784, 0.814) and 0.771 (0.755, 0.788) for PhenoAge and CA, respectively. Similarly, PAI had 1-, 3-, and 6-year interval AUCs of 0.839 (95% CI: 0.782, 0.887), 0.819 (0.794, 0.842), and 0.806 (0.787, 0.823), respectively, consistently outperforming PhenoAge (0.825 [0.772, 0.876], 0.810 [0.785, 0.834], and 0.790 [0.773, 0.808], respectively) and CA (0.756 [0.684, 0.822], 0.766 [0.738, 0.794], and 0.766 [0.747, 0.784], respectively). We noted that PAI, PhenoAge, and CA generally predicted mortality with higher C-indices and AUCs in females than in males (Table 3), but PAI showed better improvement over CA in males ($\Delta C = 0.059$) than in females

Table 2 Nonlinear and linear associations between clinical biomarkers and mortality

Biomarker	Nonlinear association		Linear association	
	Chi-square	*P* [a]	HR per SD (95% CI)	*P* [a]
log AST	172.5	**2.1×10^{-39}**	1.10 (1.04, 1.15)	**1.6×10^{-4}**
log BUN	85.7	**2.1×10^{-20}**	1.15 (1.10, 1.21)	**7.3×10^{-9}**
MCV	73.8	**8.5×10^{-18}**	1.07 (1.02, 1.12)	0.008
MCH	70.3	**5.2×10^{-17}**	1.08 (1.02, 1.13)	0.003
log ALT	62.9	**2.2×10^{-15}**	0.99 (0.95, 1.04)	0.784
RBC	57.9	**2.8×10^{-14}**	0.96 (0.92, 1.01)	0.096
SCR	55.4	**1.0×10^{-13}**	1.24 (1.18, 1.29)	**7.9×10^{-21}**
HCT	53.8	**2.2×10^{-13}**	0.99 (0.94, 1.03)	0.591
PLT	53.1	**3.1×10^{-13}**	0.98 (0.93, 1.03)	0.361
HDL-C	50.8	**1.0×10^{-12}**	0.95 (0.90, 1.00)	0.039
HGB	49.0	**2.5×10^{-12}**	1.00 (0.95, 1.04)	0.860
DBIL	41.2	**1.4×10^{-10}**	1.24 (1.18, 1.30)	**1.2×10^{-19}**
FBG	36.5	**1.5×10^{-9}**	1.23 (1.18, 1.28)	**1.1×10^{-25}**
PCT	36.1	**1.8×10^{-9}**	0.97 (0.93, 1.02)	0.254
TC	36.0	**2.0×10^{-9}**	0.90 (0.86, 0.94)	**6.1×10^{-6}**
LDL-C	33.5	**7.0×10^{-9}**	0.90 (0.86, 0.95)	**2.9×10^{-5}**
LYM	25.9	**3.6×10^{-7}**	0.82 (0.78, 0.86)	**1.0×10^{-16}**
NEUT	25.8	**3.9×10^{-7}**	1.17 (1.11, 1.22)	**1.3×10^{-10}**
log ALP	18.4	**1.8×10^{-5}**	1.20 (1.15, 1.25)	**7.8×10^{-15}**
SUA	15.9	**6.8×10^{-5}**	1.14 (1.09, 1.19)	**9.2×10^{-9}**
TBIL	15.7	**7.5×10^{-5}**	1.10 (1.05, 1.16)	**4.6×10^{-5}**
WBC	15.5	**8.5×10^{-5}**	1.17 (1.12, 1.22)	**2.6×10^{-12}**
BMI	15.1	**1.0×10^{-4}**	0.94 (0.90, 0.98)	0.008
MONO	10.8	**0.001**	1.12 (1.07, 1.18)	**2.6×10^{-6}**
Waist	10.3	**0.001**	1.05 (1.01, 1.10)	0.028
log MCHC	8.5	0.004	1.04 (0.99, 1.09)	0.144
IDBIL	7.8	0.005	1.05 (1.00, 1.10)	0.052
log RDW	4.8	0.028	1.17 (1.12, 1.22)	**2.1×10^{-14}**
DBP	4.2	0.039	1.06 (1.01, 1.11)	0.010
BASO	3.3	0.071	0.95 (0.90, 0.99)	0.018
EOS	1.9	0.165	1.01 (0.96, 1.06)	0.776
log TG	1.7	0.187	0.96 (0.91, 1.01)	0.103
PP	1.6	0.206	1.11 (1.06, 1.16)	**4.1×10^{-6}**
log MPV	1.2	0.271	1.00 (0.96, 1.05)	0.843
SBP	1.1	0.291	1.13 (1.08, 1.19)	**1.2×10^{-7}**
PDW	0.1	0.761	1.02 (0.97, 1.07)	0.443

[a] $P < 0.0014$ (0.05/36) are labeled in bold

($\Delta C = 0.033$). Furthermore, PAI showed better calibration to predict 6-year survival probabilities than PhenoAge (Fig. 4A). Decision curve analysis also suggested a greater net benefit to develop intervention strategies based on PAI than PhenoAge and CA (Fig. 4B).

When predicting mortality using Cox models with CA and ΔPAI as predictors, we estimated the HR per SD increase in ΔPAI to be 1.77 (1.68, 1.87) in the full testing set, and 1.76 (1.61, 1.92) and 1.72 (1.61, 1.84) in females and males, respectively. When further including ΔPhenoAge in the model, the HRs remained statistically significant for ΔPAI, but insignificant for ΔPhenoAge (Additional file 1: Table S7). Finally, we showed that ΔPAI performed substantially better to predict mortality than any single biomarkers in terms of C-index and AUC, even when we modeled the nonlinear effects of biomarkers using fractional polynomials (Fig. 4C–D, Additional file 1: Table S8).

Results presented above remained similar when we accounted for hospital variability using mixed-effect Cox models (Additional file 1: Tables S9–S10).

Prediction of incident CVD in the DFTJ cohort

We further evaluated whether ΔPAI could improve the prediction of incident CVD over CA (Fig. 5). We found that ΔPAI was significantly associated with incident CVD and its subtypes (IHD, ACS, and stroke). HRs per SD increase in ΔPAI were 1.18 (95% CI: 1.13, 1.24), 1.13 (1.07, 1.18), 1.22 (1.12, 1.34), and 1.40 (1.28, 1.52) for incident CVD, IHD, ACS, and stroke, respectively. Moreover, samples in the highest quartile of PAI had much higher CVD risks than those in the lowest quartile, especially for stroke (HR = 2.35 [1.76, 3.13]). When we further adjusted for 11 traditional risk factors (see Methods), the effect sizes of ΔPAI were attenuated, but remained statistically significant in CVD, ACS, and stroke (Fig. 5, Additional file 1: Table S11).

Prediction of mortality and major chronic diseases in the UK Biobank

Baseline characteristics of UKB samples are presented in Additional file 1: Table S12. Because of the difference in age and ethnicity, we observed significant differences between UKB and DFTJ participants in almost all clinical biomarkers ($P < 0.05$, Additional file 1: Table S13). Despite these differences, we also confirmed that PAI could significantly improve mortality risk prediction over CA in UKB, with C-index increased from 0.706 (0.702, 0.709) to 0.749 (0.746, 0.752). Compared to PhenoAge, PAI showed better performance in both discrimination and calibration (Additional file 1: Table S14 and Fig. S10A–B). After regressing on CA, ΔPAI has a mean of 0 and a SD of 0.46 in the UKB. The HRs per SD increase in ΔPAI were 1.61 (1.59, 1.63), 1.55 (1.52, 1.58), and 1.59 (1.57, 1.61) in all samples, females, and males, respectively (Additional file 1: Table S15). Consistent with results in DFTJ, ΔPAI performed much better than any of the 17 biomarkers to predict mortality in UKB (Additional file 1: Fig. S10C–D).

We further evaluated the prediction value of ΔPAI on the incident risks of nine major chronic diseases (Fig. 6A). We found significant associations between ΔPAI and all nine diseases, with the strongest associations found in chronic kidney disease (HR = 1.59 [1.58, 1.61]) and

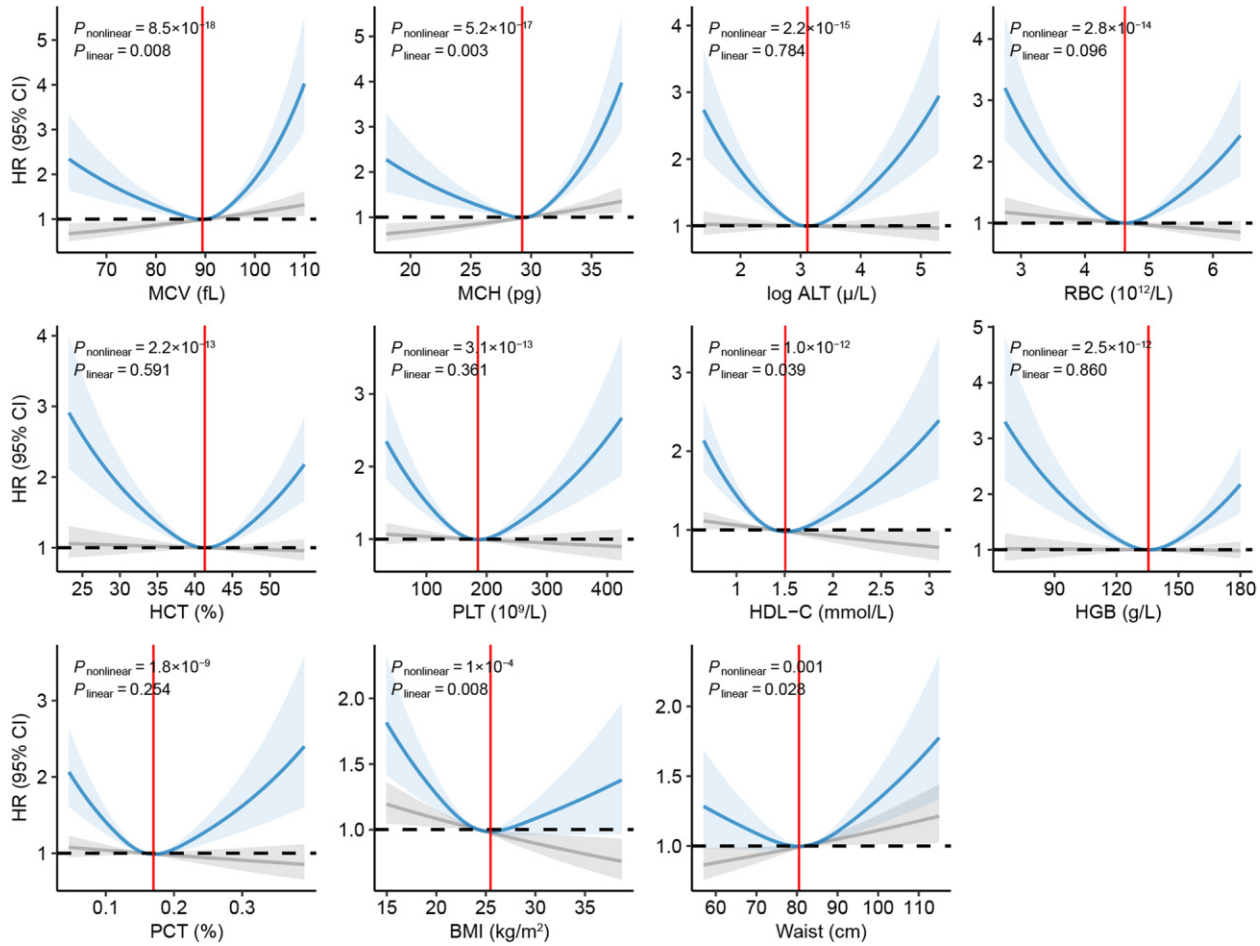

Fig. 2 Associations with mortality for biomarkers with significant nonlinear but insignificant linear relationships. HRs and CIs in linear associations, represented by grey and the shaded areas, were estimated using Cox regressions. HRs and CIs in nonlinear associations, represented by blue and the shaded areas, were estimated using Cox models with cubic splines, adjusted for CA. The mean value of each biomarker was set as the reference to calculate HR. The vertical red line indicates the optimal level corresponding to the lowest HR in the RCS curve. *P* values from both nonlinear and linear models were listed at every panel

chronic liver disease (HR = 1.48 [1.45, 1.50]). Remarkably, both ΔPAI and ΔPhenoAge, as integrative aging indices, performed better than any single biomarkers to predict eight out of nine diseases, with the only exception of diabetes. It was unsurprising that blood glucose had the highest predictive value on diabetes. Compared to ΔPhenoAge, ΔPAI performed better on the prediction of eight diseases, except for cancers, with a noticeable improvement on stroke and dementias (Fig. 6B).

Discussion

In this study, we proposed PAI to measure an individual's physiological age based on routine clinical biomarkers. While chronological age is an important risk factor for mortality and chronic diseases, we showed that PAI can significantly improve risk prediction of mortality in both the DFTJ cohort and UKB. The accelerated aging, defined as higher ΔPAI, is a risk factor of incident CVD and its subtypes in the DFTJ cohort, as well as nine major chronic diseases in the UKB. Furthermore, ΔPAI performed better than any single biomarker in the risk prediction of most diseases, highlighting the potential of PAI and ΔPAI to help identify individuals at high risk of age-related diseases for early prevention and intervention.

PAI was trained by predicting mortality from an initial set of 36 clinical biomarkers in the DFTJ cohort of elderly Chinese. While many aging clocks have been developed to predict CA [9, 11], it has been suggested that aging clocks trained with survival risks, often referred to as second-generation aging clocks, are better in gauging the aging rates [16]. For example, PhenoAge [4], which was constructed using CA and nine biomarkers from European samples, has been shown to effectively predict CVD, cancers, and other age-related diseases [47–50]. Similarly, Deelen et al. introduced a second-generation aging clock using 14 metabolites based on 44,168 European samples

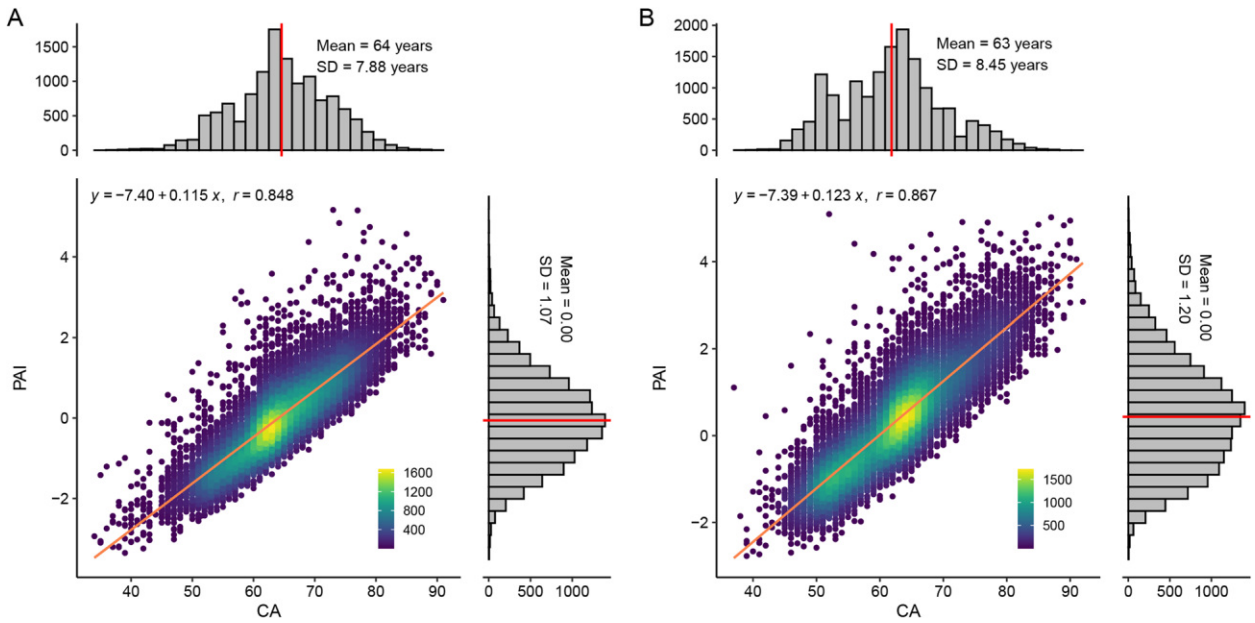

Fig. 3 Joint distribution of PAI and CA. **A** Training set. **B** Testing set. Distributions of CA and standardized PAI are shown on the top side and in the right of each panel, respectively. The point density is represented by color. The red line represents the mean value of CA or PAI. The orange line represents the linear fitting line of PAI on CA

Table 3 Evaluation of discrimination and calibration for PAI, PhenoAge, and CA in the DFTJ testing set

Evaluation metric		PAI	PhenoAge	CA
Full set				
C-index		0.816 (0.802, 0.831)	0.799 (0.784, 0.814)	0.771 (0.755, 0.788)
AUC	1-year	0.839 (0.782, 0.887)	0.825 (0.772, 0.876)	0.756 (0.684, 0.822)
	3-year	0.819 (0.794, 0.842)	0.810 (0.785, 0.834)	0.766 (0.738, 0.794)
	6-year	0.806 (0.787, 0.823)	0.790 (0.773, 0.808)	0.766 (0.747, 0.784)
Calibration	Slope	1.02 (0.97, 1.06)	1.31 (1.19, 1.43)	1.01 (0.95, 1.08)
	Intercept	−0.02 (−0.06, 0.03)	−0.30 (−0.41, −0.19)	−0.01 (−0.07, 0.05)
Only female				
C-index		0.840 (0.815, 0.866)	0.825 (0.799, 0.852)	0.807 (0.778, 0.835)
AUC	1-year	0.899 (0.838, 0.949)	0.906 (0.858, 0.943)	0.809 (0.710, 0.893)
	3-year	0.840 (0.801, 0.878)	0.844 (0.804, 0.881)	0.786 (0.736, 0.832)
	6-year	0.855 (0.828, 0.880)	0.836 (0.804, 0.864)	0.823 (0.795, 0.850)
Calibration	Slope	1.06 (1.02, 1.10)	1.51 (1.38, 1.64)	1.03 (0.99, 1.08)
	Intercept	−0.06 (−0.10, −0.02)	−0.50 (−0.62, −0.37)	−0.03 (−0.08, 0.01)
Only male				
C-index		0.759 (0.737, 0.781)	0.735 (0.712, 0.758)	0.700 (0.676, 0.725)
AUC	1-year	0.763 (0.660, 0.851)	0.714 (0.615, 0.807)	0.678 (0.572, 0.790)
	3-year	0.774 (0.734, 0.809)	0.750 (0.712, 0.787)	0.713 (0.672, 0.754)
	6-year	0.738 (0.712, 0.763)	0.718 (0.690, 0.746)	0.683 (0.655, 0.713)
Calibration	Slope	1.02 (0.95, 1.09)	1.27 (1.17, 1.37)	1.00 (0.91, 1.08)
	Intercept	−0.02 (−0.08, 0.05)	−0.25 (−0.34, −0.16)	0.01 (−0.08, 0.09)

All estimates were presented as mean (95% CI)

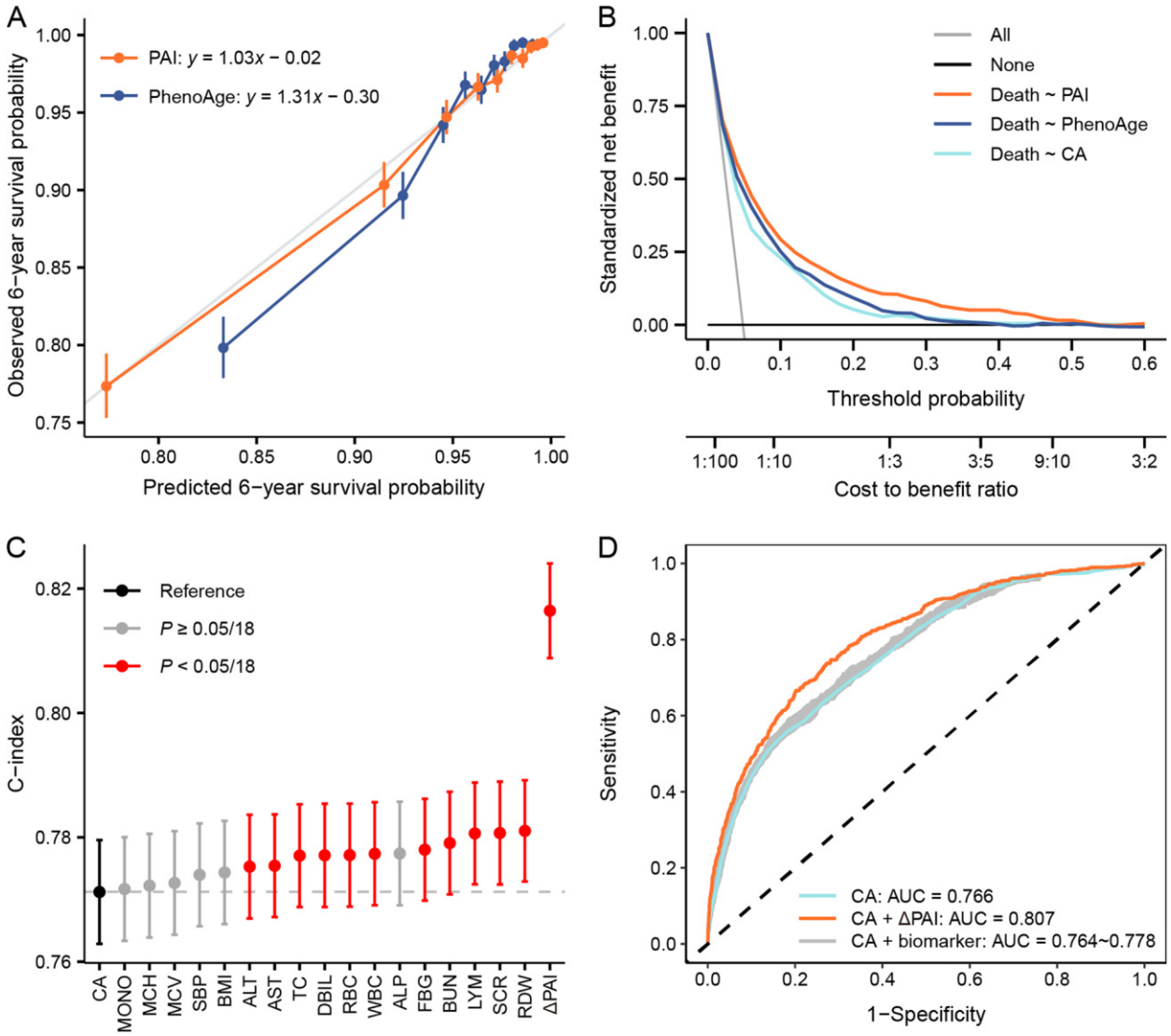

Fig. 4 Prediction of mortality using PAI and ΔPAI in the DFTJ testing set. **A** Calibration plot of the predicted and mean observed 6-year survival probability within each decile group, defined by the predicted 6-year survival probability. Vertical lines show the 95% CIs of the observed 6-year survival probability. Calibration slopes and intercepts are labeled in the equations in the legend. The grey line shows a perfect calibration scenario along the diagonal ($y = x$). **B** Decision curve analysis of mortality prediction models based on PAI, PhenoAge, and CA. For comparison, the grey and black lines indicate strategies assuming all or no individuals are treated. **C** C-index of models with CA as the only covariate (reference), as well as CA and biomarker/ΔPAI as covariates. Each dot indicates the C-index estimate, with vertical lines showing one standard error. The dashed line represents the C-index of the reference model. Models showing significant improvement over the reference model ($P < 0.05/18$) are highlighted in red. **D** The ROC curves at 6-year interval of models with CA (blue), CA and ΔPAI (orange), or CA and single biomarker (grey) as covariates

[51]. Kuo et al. developed a proteomic aging clock (PAC) based on all-cause mortality risk in UKB participants and showed that PAC performed better than PhenoAge to predict mortality [52]. Compared to the omics-based second-generation clocks, PAI offers an advantage of accessibility by utilizing routine clinical biomarkers, enabling quick evaluation of physiological age following a routine physical examination. This cost-effective feature is particularly important to facilitate the implementation of public health programs in the general population.

Previous aging clocks typically assumed linear associations between biomarkers and mortality, ignoring the predominant U-shaped relationships observed for many clinical biomarkers[16–18]. In contrast, PAI was designed to account for the nonlinear relationships by identifying the optimal level for each biomarker and modeling the effects separately for values below and above the optimal level. By effectively capturing the nonlinear relationships, PAI showed a higher predictive value of mortality and major chronic diseases than both CA and PhenoAge.

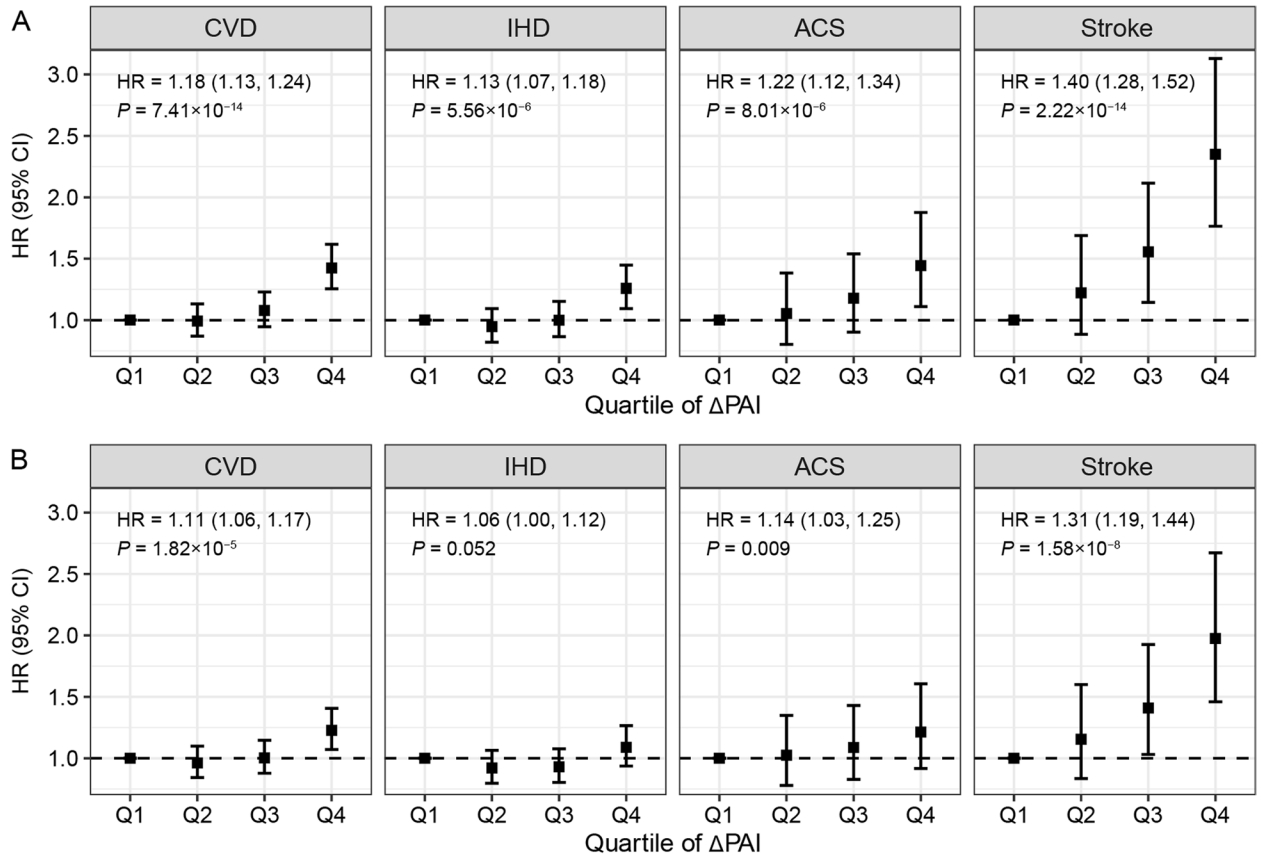

Fig. 5 HRs of ΔPAI on incident CVD and its subtypes. **A** Base model with only CA as a covariate. **B** Full model with CA and other traditional risk factors of CVD as the covariates. The black squares represent dot estimates of HRs, and the vertical lines represent 95% CIs. HR per SD increases in ΔPAI and the corresponding *P* values are listed at the top-left of each panel

Remarkably, despite being trained using the DFTJ cohort of elderly Chinese, PAI has demonstrated superior performance in the prediction of mortality and several age-related diseases in the UKB. These two cohorts present substantial differences in their sample collection and experimental protocols, baseline characteristics, genetic backgrounds, and environmental exposures. PAI outperformed PhenoAge, which was trained in European samples, in both discrimination and calibration in the prediction of mortality. Furthermore, ΔPAI outperformed ΔPhenoAge and any single biomarker in the prediction of incident IHD, stroke, COPD, dementias, CKD, hearing loss, and chronic liver diseases. The successful validation across distinct cohorts demonstrated the robustness and applicability of PAI and ΔPAI to assess physiological aging.

There are several limitations in this study. First, PAI was derived from a limited set of clinical biomarkers available in routine physical examinations. Thus, PAI might not capture the full spectrum of physiological aging. Second, ΔPAI was trained to measure accelerated aging based on clinical measurements at a single time point from the same cohort and thus might be confounded by unmeasured factors such as early-life diseases and cohort effects. Third, PAI was trained and tested in different datasets from the same cohort of elderly Chinese. While we have externally validated PAI in UKB, further validation should be performed in other Chinese cohorts, especially in those with a broader age range.

(See figure on next page.)

Fig. 6 Prediction value of ΔPAI, ΔPhenoAge, and single biomarker on mortality risk in the UKB. **A** HRs per SD increase of ΔPAI on nine major chronic diseases in the UKB. HRs of ΔPAI were estimated in Cox models with CA, smoking, drinking, obesity status, and the Townsend index as covariates. No. cases (%) indicates the number of cases (percentage) for each disease. **B** Model comparison for predicting nine major chronic diseases in the UKB. The reference model, which includes CA, sex, smoking, drinking, obesity status, and the Townsend index, is colored in black. Dots represent the C-index estimates, and vertical lines denote one standard error. The dashed line illustrates the C-index of the reference model. Models that show significant increases of C-index over the reference model are colored in red ($P < 0.05/19$)

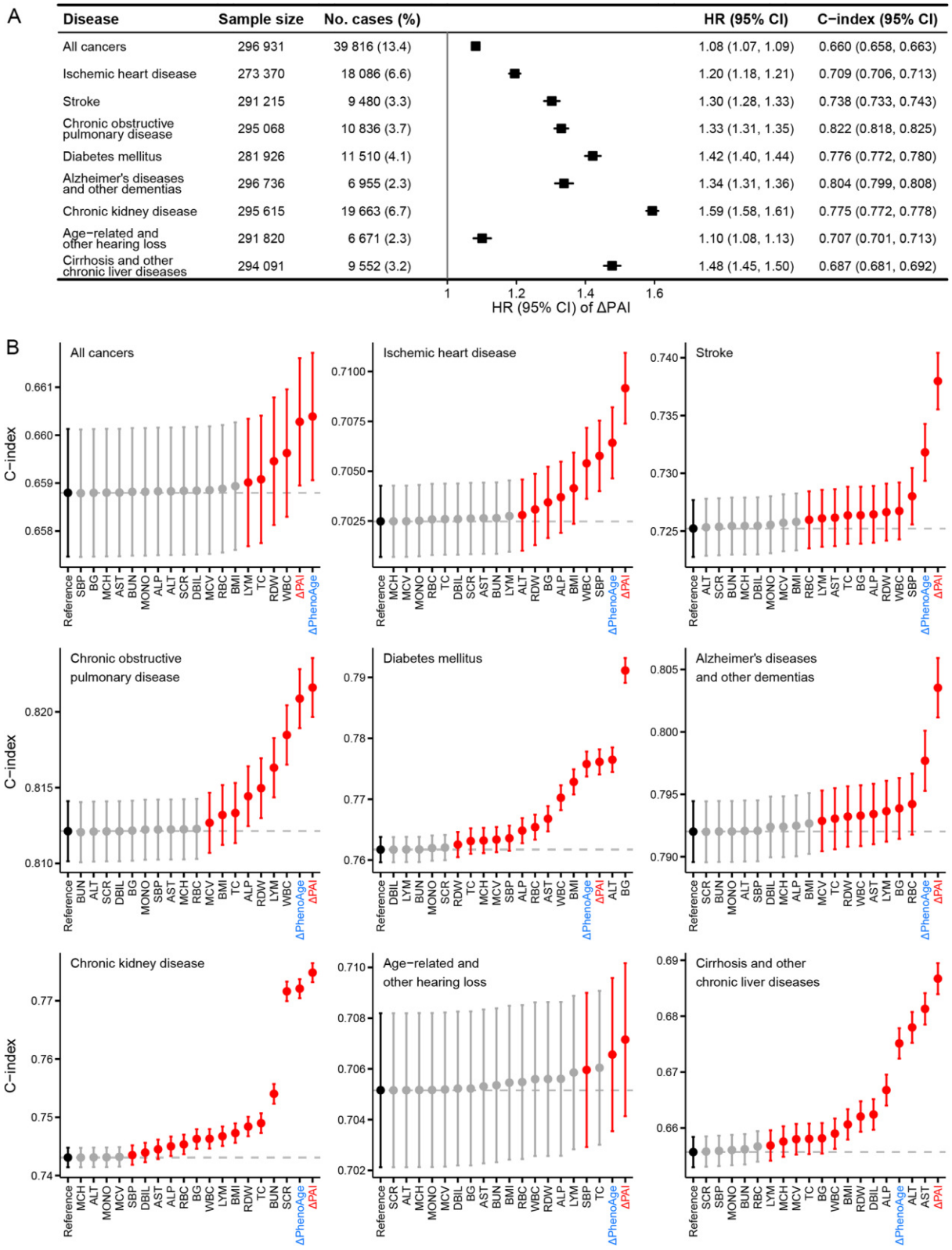

Fig. 6 (See legend on previous page.)

Conclusions

PAI and ΔPAI are cost-effective novel biomarkers to measure physiological aging and to help identify individuals at risk of accelerated aging. These indices have great potential to facilitate the development of precision intervention strategies for healthy aging. Future studies are required to assess the clinical utility of PAI.

Abbreviations

ACS	Acute coronary syndrome
AUC	Area under the receiver operator characteristic curve
BA	Biological age
C-index	Concordance index
CA	Chronological age
CKB	China Kadoorie Biobank
CKD	Chronic kidney disease
COPD	Chronic obstructive pulmonary disease
CVD	Cardiovascular diseases
DALY	Disability-adjusted life-year
DBIL	Direct bilirubin
DFTJ	Dongfeng-Tongji
HR	Hazard ratio
ICD-10	International classification of diseases tenth revision
IHD	Ischemic heart disease
KDM	Klemera and Doubal's method
PAC	Proteomic aging clock
PAI	Physiological aging index
PP	Pressure pulse
RCS	Restricted cubic spline
RDW	Red cell volume distribution width
ROC	Receiver operator characteristic
SBP	Systolic blood pressure
SD	Standard deviation
TS index	Townsend index
UKB	UK Biobank

Supplementary Information

The online version contains supplementary material available at https://doi.org/10.1186/s12916-024-03769-2.

Supplementary Material 1. Additional file 1: Table S1. Characteristic of 36 clinical biomarkers in this study. Table S2. Definition of cardiovascular diseases in the DFTJ cohort. Table S3. Model weights of PhenoAge calculation. Table S4. Comparison of biomarkers among different hospitals in the DFTJ cohort. Table S5. Definition of major chronic diseases in the UKB. Table S6. Model weights of PAI calculation. Table S7. HRs of ΔPAI and ΔPhenoAge on mortality in the DFTJ testing set. Table S8. Predictive performance of single biomarker in the DFTJ testing set. Table S9. Predictive performance of mortality in the DFTJ testing set using mixed-effect Cox model. Table S10. HRs of ΔPAI and ΔPhenoAge on mortality in the DFTJ testing set using mixed-effect Cox model. Table S11. Associations between ΔPAI and incident CVD and its subtypes. Table S12. Basic characteristics of the UKB. Table S13. Comparison of biomarkers between DFTJ cohort and the UKB. Table S14. Evaluation of discrimination and calibration for PAI, PhenoAge, and CA in the UKB. Table S15. HRs of ΔPAI and ΔPhenoAge on mortality in the UKB. Figure S1. Timeline of the DFTJ cohort and flowchart of study participants. Figure S2. Quality control process in the DFTJ training dataset. Figure S3. Summary of quality control in the DFTJ training set. Figure S4. Quality control process in the DFTJ testing dataset. Figure S5. Summary of quality control in the DFTJ testing set. Figure S6. Joint distribution of CA and sex in the DFTJ testing set. Figure S7 Missing proportion and the number of samples with outlier in the UKB. Figure S8. Nonlinear and linear associations between 25 clinical biomarkers and mortality in the DFTJ cohort. Figure S9. Regularization parameter (lambda) selection in cross validation. Figure S10. Prediction of mortality using PAI and ΔPAI in the UKB.

Acknowledgements

The authors thank all individuals who participated in this study.

Authors' contribution

CW, SC, and ZZ designed the study. ZZ and JL cleaned and analyzed data. XH, HG, XZ, and MH contributed data. ZZ drafted the paper with input from CW, SC, JL, XH, and XC. All authors read and approved the manuscript.

Funding

This work was funded by the Natural Science Foundation of China (82325044 and 82021005), the Noncommunicable Chronic Diseases-National Science and Technology Major Project (2023ZD0509900), and the Fundamental Research Funds for the Central Universities (HUST: 2019kfyXJJS036, 2023BR030, YCJJ20230248). The Natural Science Fund for Distinguished Young Scholars of Hubei Province (2022CFA046). The UK Biobank data were accessed under the Application ID 88159.

Data availability

The DFTJ data are available through reasonable request to the corresponding authors. For the UK Biobank dataset, researchers registered with the UK Biobank can apply for access to the UK Biobank Resource.

Declarations

Ethics approval and consent to participate

All participants from the Dongfeng-Tongji cohort provided written informed consent. The study protocol was approved by the Medical Ethics Committee of Tongji Medical College, Huazhong University of Science and Technology (2012–10).

Consent for publication

Not applicable.

Competing interests

The authors declare no competing interests.

Author details

[1]Ministry of Education Key Laboratory of Environment and Health, School of Public Health, Tongji Medical College, Huazhong University of Science and Technology, Wuhan, China. [2]Department of Epidemiology and Biostatistics, School of Public Health, Tongji Medical College, Huazhong University of Science and Technology, Wuhan, China. [3]Department of Occupational and Environmental Health, School of Public Health, Tongji Medical College, Huazhong University of Science and Technology, Wuhan, China. [4]Department of Cardiology, Union Hospital, Tongji Medical College, Huazhong University of Science and Technology, Wuhan, China.

Received: 28 March 2024 Accepted: 13 November 2024
Published online: 22 November 2024

References

1. Beard JR, Officer A, de Carvalho IA, Sadana R, Pot AM, Michel JP, et al. The world report on ageing and health: a policy framework for healthy ageing. Lancet. 2016;387:2145–54.
2. Partridge L, Deelen J, Slagboom PE. Facing up to the global challenges of ageing. Nature. 2018;561:45–56.
3. Lu AT, Quach A, Wilson JG, Reiner AP, Aviv A, Raj K, et al. DNA methylation GrimAge strongly predicts lifespan and healthspan. Aging (Albany NY). 2019;11:303–27.
4. Levine ME, Lu AT, Quach A, Chen BH, Assimes TL, Bandinelli S, et al. An epigenetic biomarker of aging for lifespan and healthspan. Aging (Albany NY). 2018;10:573–91.
5. Belsky DW, Caspi A, Arseneault L, Baccarelli A, Corcoran DL, Gao X, et al. Quantification of the pace of biological aging in humans through a blood test, the DunedinPoAm DNA methylation algorithm. Elife. 2020;9:e54870.
6. Horvath S. DNA methylation age of human tissues and cell types. Genome Biol. 2013;14:R115.

7. Sayed N, Huang Y, Nguyen K, Krejciova-Rajaniemi Z, Grawe AP, Gao T, et al. An inflammatory aging clock (iAge) based on deep learning tracks multimorbidity, immunosenescence, frailty and cardiovascular aging. Nat Aging. 2021;1:598–615.
8. Fleischer JG, Schulte R, Tsai HH, Tyagi S, Ibarra A, Shokhirev MN, et al. Predicting age from the transcriptome of human dermal fibroblasts. Genome Biol. 2018;19:221.
9. Hertel J, Friedrich N, Wittfeld K, Pietzner M, Budde K, Van der Auwera S, et al. Measuring biological age via metabonomics: the metabolic age score. J Proteome Res. 2016;15:400–10.
10. Pyrkov TV, Avchaciov K, Tarkhov AE, Menshikov LI, Gudkov AV, Fedichev PO. Longitudinal analysis of blood markers reveals progressive loss of resilience and predicts human lifespan limit. Nat Commun. 2021;12:2765.
11. Putin E, Mamoshina P, Aliper A, Korzinkin M, Moskalev A, Kolosov A, et al. Deep biomarkers of human aging: application of deep neural networks to biomarker development. Aging (Albany NY). 2016;8:1021–33.
12. Hannum G, Guinney J, Zhao L, Zhang L, Hughes G, Sadda S, et al. Genome-wide methylation profiles reveal quantitative views of human aging rates. Mol Cell. 2013;49:359–67.
13. Klemera P, Doubal S. A new approach to the concept and computation of biological age. Mech Ageing Dev. 2006;127:240–8.
14. Levine ME. Modeling the rate of senescence: can estimated biological age predict mortality more accurately than chronological age? J Gerontol A Biol Sci Med Sci. 2013;68:667–74.
15. Chen L, Zhang Y, Yu C, Guo Y, Sun D, Pang Y, et al. Modeling biological age using blood biomarkers and physical measurements in Chinese adults. EBioMedicine. 2023;89: 104458.
16. Galkin F, Mamoshina P, Aliper A, de Magalhaes JP, Gladyshev VN, Zhavoronkov A. Biohorology and biomarkers of aging: current state-of-the-art, challenges and opportunities. Ageing Res Rev. 2020;60: 101050.
17. Nelson PG, Promislow DEL, Masel J. Biomarkers for Aging Identified in Cross-sectional Studies Tend to Be Non-causative. J Gerontol A Biol Sci Med Sci. 2020;75:466–72.
18. Sluiskes MH, Goeman JJ, Beekman M, Slagboom PE, Putter H, Rodriguez-Girondo M. Clarifying the biological and statistical assumptions of cross-sectional biological age predictors: an elaborate illustration using synthetic and real data. BMC Med Res Methodol. 2024;24:58.
19. Khramtsova EA, Davis LK, Stranger BE. The role of sex in the genomics of human complex traits. Nat Rev Genet. 2019;20:173–90.
20. Bhaskaran K, Dos-Santos-Silva I, Leon DA, Douglas IJ, Smeeth L. Association of BMI with overall and cause-specific mortality: a population-based cohort study of 3.6 million adults in the UK. Lancet Diabetes Endocrinol. 2018;6:944–53.
21. Cho SK, Chang Y, Kim I, Ryu S. U-Shaped Association Between Serum Uric Acid Level and Risk of Mortality: A Cohort Study. Arthritis Rheumatol. 2018;70:1122–32.
22. Vinholt PJ, Hvas AM, Frederiksen H, Bathum L, Jorgensen MK, Nybo M. Platelet count is associated with cardiovascular disease, cancer and mortality: A population-based cohort study. Thromb Res. 2016;148:136–42.
23. Wang F, Zhu J, Yao P, Li X, He M, Liu Y, et al. Cohort profile: the Dongfeng-Tongji cohort study of retired workers. Int J Epidemiol. 2013;42:731–40.
24. Gao M, Lv J, Yu C, Guo Y, Bian Z, Yang R, et al. Metabolically healthy obesity, transition to unhealthy metabolic status, and vascular disease in Chinese adults: a cohort study. PLoS Med. 2020;17: e1003351.
25. Han X, Wei Y, Hu H, Wang J, Li Z, Wang F, et al. Genetic risk, a healthy lifestyle, and type 2 diabetes: the Dongfeng-Tongji cohort study. J Clin Endocrinol Metab. 2020;105:dgz325.
26. Eckel RH, Jakicic JM, Ard JD, de Jesus JM, Houston Miller N, Hubbard VS, et al. 2013 AHA/ACC guideline on lifestyle management to reduce cardiovascular risk: a report of the American College of Cardiology/American Heart Association Task Force on Practice Guidelines. J Am Coll Cardiol. 2014;63:2960–84.
27. Lu Q, Zhang Y, Geng T, Yang K, Guo K, Min X, et al. Association of lifestyle factors and antihypertensive medication use with risk of all-cause and cause-specific mortality among adults with hypertension in China. JAMA Netw Open. 2022;5:e2146118.
28. Jensen MD, Ryan DH, Apovian CM, Ard JD, Comuzzie AG, Donato KA, et al. 2013 AHA/ACC/TOS guideline for the management of overweight and obesity in adults: a report of the American College of Cardiology/American Heart Association Task Force on Practice Guidelines and The Obesity Society. Circulation. 2014;129:S102–38.
29. Chang AY, Skirbekk VF, Tyrovolas S, Kassebaum NJ, Dieleman JL. Measuring population ageing: an analysis of the Global Burden of Disease Study 2017. Lancet Public Health. 2019;4:e159–67.
30. GBD 2021 Diseases and Injuries Collaborator. Global incidence, prevalence, years lived with disability (YLDs), disability-adjusted life-years (DALYs), and healthy life expectancy (HALE) for 371 diseases and injuries in 204 countries and territories and 811 subnational locations, 1990–2021: a systematic analysis for the Global Burden of Disease Study 2021. Lancet. 2024;403:2133–61.
31. Janca A, Ustun TB, Early TS, Sartorius N. The ICD-10 symptom checklist: a companion to the ICD-10 classification of mental and behavioural disorders. Soc Psychiatry Psychiatr Epidemiol. 1993;28:239–42.
32. He S, Lei W, Li J, Yu K, Yu Y, Zhou L, et al. Relation of platelet parameters with incident cardiovascular disease (the Dongfeng-Tongji cohort study). Am J Cardiol. 2019;123:239–48.
33. Diao T, Liu K, Wang Q, Lyu J, Zhou L, Yuan Y, et al. Bedtime, sleep pattern, and incident cardiovascular disease in middle-aged and older Chinese adults: The dongfeng-tongji cohort study. Sleep Med. 2023;110:82–8.
34. Luepker RV, Apple FS, Christenson RH, Crow RS, Fortmann SP, Goff D, et al. Case definitions for acute coronary heart disease in epidemiology and clinical research studies: a statement from the AHA Council on Epidemiology and Prevention; AHA Statistics Committee; World Heart Federation Council on Epidemiology and Prevention; the European Society of Cardiology Working Group on Epidemiology and Prevention; Centers for Disease Control and Prevention; and the National Heart, Lung, and Blood Institute. Circulation. 2003;108:2543–9.
35. Li P, Stuart EA, Allison DB. Multiple imputation: a flexible tool for handling missing data. JAMA. 2015;314:1966–7.
36. Heinzl H, Kaider A. Gaining more flexibility in Cox proportional hazards regression models with cubic spline functions. Comput Methods Programs Biomed. 1997;54:201–8.
37. Simon N, Friedman J, Hastie T, Tibshirani R. Regularization paths for Cox's proportional hazards model via coordinate descent. J Stat Softw. 2011;39:1–13.
38. Longato E, Vettoretti M, Di Camillo B. A practical perspective on the concordance index for the evaluation and selection of prognostic time-to-event models. J Biomed Inform. 2020;108:103496.
39. Hung H, Chiang CT. Estimation methods for time-dependent AUC models with survival data. Can J Stat. 2010;38:8–26.
40. Steyerberg EW, Vergouwe Y. Towards better clinical prediction models: seven steps for development and an ABCD for validation. Eur Heart J. 2014;35:1925–31.
41. Van Calster B, Wynants L, Verbeek JFM, Verbakel JY, Christodoulou E, Vickers AJ, et al. Reporting and Interpreting decision curve analysis: a guide for Investigators. Eur Urol. 2018;74:796–804.
42. Vickers AJ, Elkin EB. Decision curve analysis: a novel method for evaluating prediction models. Med Decis Making. 2006;26:565–74.
43. Royston P, Ambler G, Sauerbrei W. The use of fractional polynomials to model continuous risk variables in epidemiology. Int J Epidemiol. 1999;28:964–74.
44. Kang L, Chen W, Petrick NA, Gallas BD. Comparing two correlated C indices with right-censored survival outcome: a one-shot nonparametric approach. Stat Med. 2015;34:685–703.
45. Sudlow C, Gallacher J, Allen N, Beral V, Burton P, Danesh J, et al. UK biobank: an open access resource for identifying the causes of a wide range of complex diseases of middle and old age. PLoS Med. 2015;12:e1001779.
46. Kuo CL, Pilling LC, Liu Z, Atkins JL, Levine ME. Genetic associations for two biological age measures point to distinct aging phenotypes. Aging Cell. 2021;20: e13376.
47. Cao X, Zhang J, Ma C, Li X, Kuo CL, Levine ME, et al. Life course traumas and cardiovascular disease-the mediating role of accelerated aging. Ann N Y Acad Sci. 2022;1515:208–18.
48. Deryabin PI, Borodkina AV. Epigenetic clocks provide clues to the mystery of uterine ageing. Hum Reprod Update. 2023;29:259–71.
49. Faul JD, Kim JK, Levine ME, Thyagarajan B, Weir DR, Crimmins EM. Epigenetic-based age acceleration in a representative sample of older Americans: associations with aging-related morbidity and mortality. Proc Natl Acad Sci U S A. 2023;120:e2215840120.

50. Mak JKL, McMurran CE, Kuja-Halkola R, Hall P, Czene K, Jylhava J, et al. Clinical biomarker-based biological aging and risk of cancer in the UK Biobank. Br J Cancer. 2023;129:94–103.
51. Deelen J, Kettunen J, Fischer K, van der Spek A, Trompet S, Kastenmuller G, et al. A metabolic profile of all-cause mortality risk identified in an observational study of 44,168 individuals. Nat Commun. 2019;10:3346.
52. Kuo CL, Chen Z, Liu P, Pilling LC, Atkins JL, Fortinsky RH, et al. Proteomic aging clock (PAC) predicts age-related outcomes in middle-aged and older adults. Aging Cell. 2024;23:e14195.

Publisher's Note